SLAC–PUB–4859
February 1989
(A/I)

WHERE DO WE STAND ON THE SLC?*

WITOLD KOZANECKI
Stanford Linear Accelerator Center, Stanford University, Stanford, California 94309

ABSTRACT: This paper reviews the current performance of the SLAC Linear Collider, as well as the issues, problems and prospects facing the project. A few of the original accelerator physics results achieved in the last year are described in detail.

*Work supported by the Department of Energy, contract DE–AC03–76SF00515.

Presented at the 8th International Conference on of Physics in Collision, Capri, Italy, October 19–21, 1988.

1. INTRODUCTION

In this paper we report on the progress of the SLAC Linear Collider (SLC),[1] the prototype of a new generation of colliding beam accelerators. This novel type of machine holds the potential of extending electron-positron colliding beam studies to center-of-mass energies far in excess of what is economically achievable with colliding beam storage rings. The same technology, if and when available at a reasonable cost, may also provide the primary charged particle beams needed to produce high energy, high luminosity photon-photon collisions.[2]

In addition to its role as a test vehicle for the linear collider principle, the SLC aims at providing a source of Z^0 decays to high energy physics experiments. Accordingly, two major detectors, the upgraded MarkII, now installed on the SLC beam line, and the more powerful SLD detector which is nearing completion, are preparing to probe the Standard Model at the Z^0 pole.

This paper reviews the current status of the SLC, and attempts to summarize the issues, problems and prospects facing the project at this time. After a brief assessment of the performance to date, we describe some of the original accelerator physics results obtained in the last year, in particular concerning the central issues of wakefield control and of the beam-beam interaction at the collision point. We conclude with an outline of the work in progress and of the outlook for the medium-term physics program.

II. MACHINE PERFORMANCE

Rather than a linear collider (Fig. 1a) in the truest sense (two linacs pointing at each other), the SLC (Fig. 1b) is an adaptation of existing SLAC facilities. The twenty-year-old Linac was considerably upgraded, damping rings were added near injection, and transport lines were appended to the end of the accelerator to bring intense, very small phase space beams into collision. Table I lists the basic SLC design parameters, the initial goals for last year's running, and the values that have been achieved in practice so far. We refer the reader to Refs. 3 and 4 and the bibliography listed therein, for a detailed description of the various subsystems.

The SLC has functioned reasonably well as a project in linear collider research and development, and already has, to a large extent, proven the feasibility of the concept. Most of the accelerator physics issues on the production of high energy, low emittance

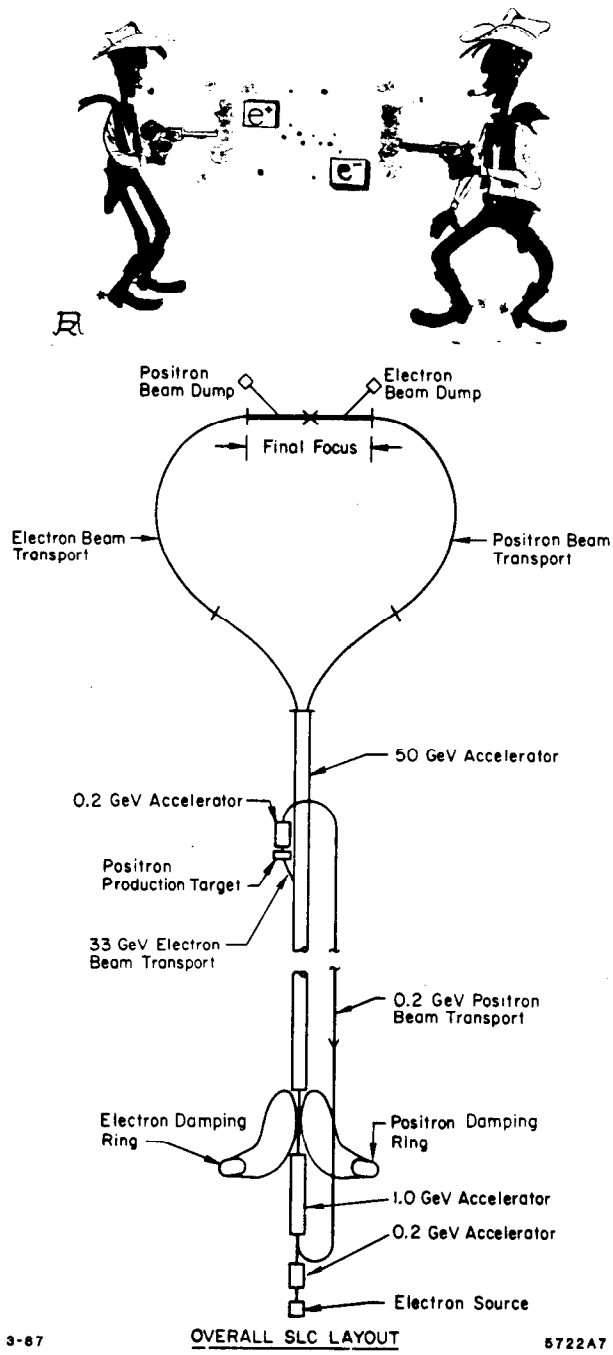

Fig. 1. Schematic layout of a linear collider: (a) concept; (b) first practical implementation: the SLC. The projectile density, the firing rate, and the aiming accuracy and stability are the critical parameters.

beams, their transport and demagnification to transverse sizes of a few microns, and the electromagnetic interactions of the two beams when brought into collision, have confirmed current theoretical expectations, at least at the moderate beam intensities achieved so far.

Table I. SLC Machine Parameters

Parameter	Design	Initial Goal	Achieved[a]
Energy (GeV)	50	47	53
Intensity ($e^{\pm}$/pulse)	7×10^{10}	$1 \cdot 10^{10}$	1×10^{10} (e^+)
			2×10^{10} (e^-)
Spot sizes (σ in μm)	1.8	4	5 (horizontal)
			3 (vertical)
Repetition rate	180	60	30
Luminosity (cm^{-2} s^{-1})	6×10^{30}	10^{27}	$\sim 10^{26}$

[a]These values have been reproducibly achieved, but not simultaneously with good efficiency.

Unfortunately, however, the machine has not yet proven to be a usable research tool for particle physics. Initial attempts in the last year met with failure because of extremely poor reliability of a number of hardware components, and of cumbersome procedures needed to set up the beams for physics. A total of thirty hours of colliding beam time, much of which suffering from excessive backgrounds, was logged by the MarkII experiment. The corresponding integrated luminosity corresponds to a 50% probability for producing a detectable Z^0. While no candidate annihilation event was found in the data sample, one two-photon event of the type $e^+e^- \rightarrow e^+e^-e^+e^-$ was uncovered.[4)]

III. COMMISSIONING PROGRESS AND ISSUES IN THE MAJOR SLC SYSTEMS

A. Sources

The electron injector[4,5)] has been fully operational and has mostly met SLC specifications for intensities up to a few 10^{10} electrons per pulse. At high currents, however, improvements are needed in the area of intensity jitter (which in turn causes energy fluctuations through varying RF loading in the Linac). Simultaneous acceleration of all three bunches (two of electrons and one of positrons) prior to injection into the Damping Ring also remains to be commissioned to allow for 120 Hz collider operation.

It is possible to tune[6)] the positron source to generate 10^{10} e^+ per pulse at the end of the linac with $\approx 2 \times 10^{10}$ electrons incident on the production target, but it is more typical to obtain a somewhat smaller yield. Power absorption limitations in the existing stationary target prevent the use of scavenger bunches with appreciably

greater intensities. Much effort will be devoted, during the early commissioning period that starts in February 1989, to a careful optimization of the source capture parameters and of the transmission in the positron line and in the first sector of the Linac. In addition, the south Linac–to–Ring (LTR) transfer line is currently being outfitted with an RF energy compressor, which is expected to increase by about 50% the input momentum acceptance of the positron ring. The combined effect of these improvements is projected to increase the overall usable positron yield by a factor of two to three. Bringing the positron current up to full SLC specifications will require the installation of a new moving target, which is presently under fabrication and is scheduled for installation in the Fall of 1989.

B. Damping Rings

Much progress has been accomplished in this area. While damping times and equilibrium vertical emittance have long since been shown to be satisfactory, deliberate coupling of the horizontal and vertical tunes has helped reduce the horizontal emittance and make the SLC, as a whole, less sensitive to parasitic cross-plane effects. The deleterious consequences of bunch lengthening and turbulent phenomena[7)] were successfully curbed, at least in part, by enlarging the aperture of the electron Ring–to–Linac (RTL) transfer line. With these improvements, a part of which is being duplicated on the positron ring, the synchrotron phase space at the output of the ring should allow operation up to 4–5 $\times$ 10^{10} particles/pulse. Reaching full design specifications may require a more extensive rework of the damping ring vacuum pipe to further reduce the impedance.

But serious problems remain. Considerable down time and beam instability problems plagued the commissioning program because of the high failure rate of the damping ring injection and extraction kickers. The basic requirements on these magnets—integrated field, rise time, fall time, flat top, repeatability of the kick—imposed by two-bunch operation and, at high intensity, by transverse wakefields, could not so far be met all simultaneously. A large-scale effort to increase the radiation hardness of the critical components and to improve the reliability and serviceability of the pulsing systems is underway. Operation has been temporarily restricted to single bunch mode (where positron production and e^+–e^- collisions occur on alternate pulses), limiting the rate at the IP to 60 Hz. Stability requirements at present intensities have been eased by the successful implementation of BNS damping. These combined measures are expected to allow satisfactory operation in the short term, while a totally new kicker design is actively being pursued.

C. Linac

In the course of SLC construction, the SLAC Linac has been upgraded[8–11] to accelerate tightly focused beams of positrons and electrons on the same RF pulse without significant emittance increase. About 230 new 67 MW klystrons[12] were installed. Beam energies of up to 53 GeV were measured. About 1.5×10^{10} electrons and 8×10^{9} positrons per pulse are now routinely accelerated to 47 GeV.

The transverse shapes of the beams at the end of the Linac depend on input trajectory and optical conditions upon injection from the RTL, on the quadrupole lattice and the energy-acceleration profile along the Linac, on the alignment of the beam with respect to the RF structure, and on transverse wakefields. In the remainder of this section, we will elaborate on some of the most important aspects of such phase space control. Only a succinct account is intended here: more details are available elsewhere in the literature.[4,13–16]

Transverse electron emittances measured at low current at the end of the Linac lie between about one (in the vertical plane) and two or three times (in the horizontal plane) the design value. After elimination of residual unmatched dispersion in the RTL (which can be tuned away empirically), the apparent horizontal emittance still undergoes a blowup of a factor of two during transport from the ring to the entrance of the Linac. Betatron mismatches have been diagnosed at the exit of the ring, and, in addition, in the RTL proper. Sophisticated data-acquisition and off-line analysis methods are being developed to map the evolution of phase space through the transport lines, using betatron oscillations deliberately induced at a complete set of phases and recorded by beam position monitors (BPMs).

Another potential source of apparent emittance growth resided in the occasional mismatch between the settings of the Linac quadrupoles and the actual longitudinal energy profile of the accelerator. As the lattice is not achromatic, relatively small energy scale errors result in sizeable accumulated phase slippages along the machine, so that the phase space ellipses corresponding to different energies within the bunch, no longer overlap. Both static and dynamic lattice-energy mismatches have been identified and corrected. The relative RF phases of individual klystrons, or of entire sectors, have been observed to drift, over periods of weeks to months, by up to 45 degrees. Experience accumulated in the last six months, however, shows that the proper phase configuration can be maintained by small periodic readjustments based on relative beam energy

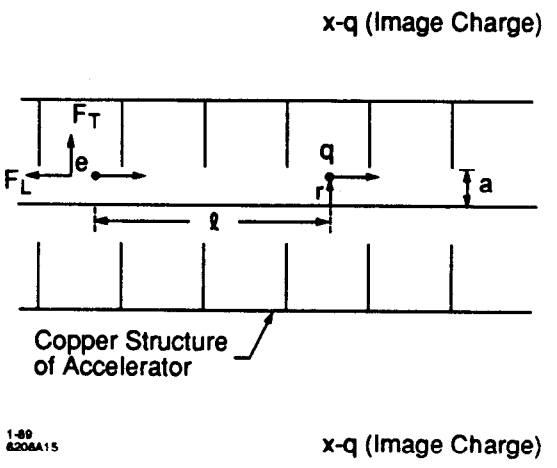

Fig. 2. Forces exerted on a test charge trailing a distance behind a charge element q by the charge element and its image charges in the disc-loaded copper accelerating structure of the SLAC linac. The test charge is taken to be the same sign as the charge element.

measurements: this is now part of weekly maintenance practice. Energy profile changes also occur on a much shorter time scale, for instance when it proves necessary to redistribute the contingent of active klystrons along the machine. The development of an "energy management" computer program, which, upon operator request, adjusts the quadrupole settings as a function of the actual klystron population, has greatly improved the optical stability of the Linac.

The dramatically increased bunch intensities and reduced emittances (compared to the old linac), have required that extreme care be taken to control the effects of the interactions between particles within each bunch, and between particles in the bunch and the accelerating structure. Growth in the energy spread of the beam and distortions in the bunch shape generated respectively by longitudinal and transverse wakefields have been controlled by tighter steering in the first two sectors of the Linac, improvements to the BPM hardware and calibration procedures, improvements in beam steering algorithms, implementation of new RF phase configurations, and by the establishment of suitable feedback networks.

As a high-intensity bunch of electrons (or positrons) travels through the disc-loaded accelerating structure, forces are exerted on individual particles not only by the externally generated RF field, but also by the remaining particles in the bunch and by their image currents in the metallic structure. Most of the qualitative features of these wakefields can be grasped from the simple quasistatic picture in Fig. 2. A test particle some distance

behind a charge element q will be decelerated by the residual longitudinal force created by q and its image charges, and if the charge element is not at the center of the waveguide, then there will be in addition a net transverse force on the test particle. For small transverse displacements ($r \ll a$), the strength of these wakefields can be written[17] in terms of potentials that depend only on the longitudinal separation l of the two charges:

$$F_L = q \cdot W_L(l) \tag{1a}$$

$$F_T = q \cdot \left(\frac{r}{a}\right) \cdot W_T(l) \tag{1b}$$

As the accelerated bunch is made shorter, the longitudinal force exerted on particles at the tail of the bunch increases. This causes the energy spread within the bunch to increase. When the intensity exceeds $\approx 10^{10}$ particles per bunch, the longitudinal head-tail interaction generates an excessively large energy spread in the beam. This can be compensated for by positioning the bunch at a phase such that the accelerating voltage is larger at the tail than at the head, but it must be done to about one degree of S-band. The RF phase needs to be continuously adjusted for long-term thermal and pressure drifts in the RF cavities and in the gas-filled timing cables.[18] In practice, the energy spread of the beam can be maintained to $\sigma_E/E \approx 0.2 - 0.3\%$ (within specifications).

On the other hand, the transverse force on the tail of the bunch grows as the bunch becomes longer. The resulting phase space distortions, which are highly non-linear and cannot be corrected further downstream, contribute both to loss of luminosity (through spot size increase) and to severe backgrounds in the experimental detector. Distortions in the bunch shape due to transverse wakefields can be minimized[13] by maintaining the beam trajectory as near to the axis of the waveguide as possible (Eq. 1b). The BPM system in the Linac, combined with presently used steering algorithms, is sufficient to simultaneously place both the e^- and the e^+ beams within 250 microns r.m.s. of the design trajectory. The effects of deliberately mis-steering the beam are shown in Fig. 3. The well-steered beam in the middle of the figure shows little distortion in the bunch shape, but if a betatron oscillation is induced with a dipole steering magnet at the beginning of the Linac, then by the time the beam reaches the end of the accelerator, the tail is displaced laterally with respect to the head by many times the intrinsic width of the bunch.

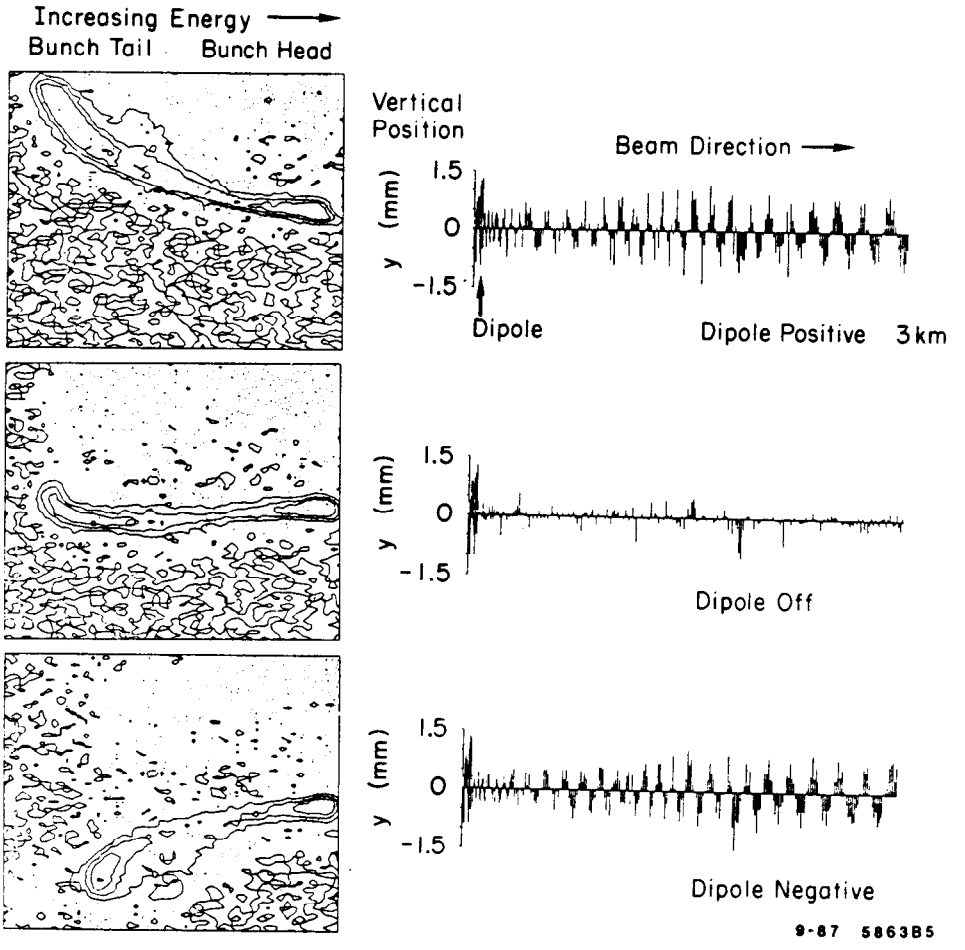

Fig. 3. Effect of deliberately mis-steering the e^- beam in the Linac. The pictures at the left side of this figure are measured contour plots of the bunch population projected into the yz plane. In the figures at the right, the displacement of the beam from the nominal centerline of the accelerator is measured at 232 locations along the 3 km length of the machine. Each measurement is plotted as a vertical line. Positive offsets are displayed by lines that extend above the axis and negative offsets by lines that extend downward. The full scale corresponds to offsets of $\pm$ 1.5 mm. The tail of the bunch (far left in the contour plot) is severely deflected with respect to the head when the beam is not maintained on axis in the accelerating structure (top and bottom pairs of figures.)

The development of the transverse head-tail distortion in the Linac depends on the energy distribution of particles in the bunch. If there were no correlation between the energy of an electron and its longitudinal position in the bunch, then as depicted in Fig. 4, any residual coherent betatron oscillation in the beam trajectory that might be induced by steering errors will result in repeated (coherent) transverse kicks to the tail of the beam. This coherence can be destroyed if the energies of particles at the tail of the bunch are made systematically different from the energies of the particles at the head,

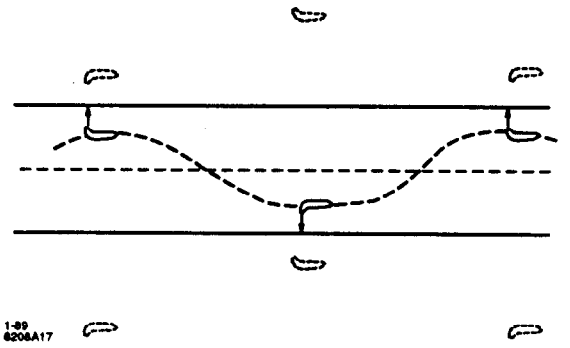

Fig. 4. Transverse wake forces on the tail of a bunch as it travels down the linac with a betatron oscillation of finite amplitude.

so that the head and the tail oscillate at different betatron frequencies. A generalization of this idea [BNS damping[19)]] takes advantage of the fact that the effective focusing strength of quadrupoles is greater for lower energy particles. Positioning the bunch with respect to the RF waveform, at a phase such that the head maintains a higher energy than the tail by about 1%, achieves both goals. This of course would increase the final energy spread to an unacceptably large value unless compensated for further down the accelerator, once the bunch has acquired enough rigidity to be less sensitive to transverse wakes. The detailed pattern of klystron phases is chosen to achieve both an acceptable energy spread and to provide control of transverse wake instabilities. This scheme has been very successfully applied,[15,16)] for the first time, in the SLAC Linac, to damp the growth of transverse instabilities for electron currents up to 2–3 $\times$ 10^{10} particles per pulse. Depending on their exact phase, oscillations initiated early in the Linac see their amplitude growth reduced by one to two orders of magnitude.[16)] The implementation of BNS damping has led to much more stable and forgiving machine operation. For example (Fig. 5), injection tolerances from the Damping Ring to the Linac are relaxed, at fixed current, by a factor of five to ten; for a given level of kicker performance (*i.e.*, at fixed injection tolerance) the maximum operating current goes up by about a factor of three.

The use of feedback to make fine adjustments to beam trajectories and timing systems is very much at the heart of the operation of the SLC. This function mostly occurs naturally in a well-designed storage ring, where only those particles that occupy the proper phase space survive beyond the first few thousand turns. In a single-pass machine, no such natural selection occurs: the beam must be mastered anew on each pulse.

Feedback loops are used, for instance, to control the incident e^- energy in the positron return line, or to adjust the electron and positron energies independently at the end of

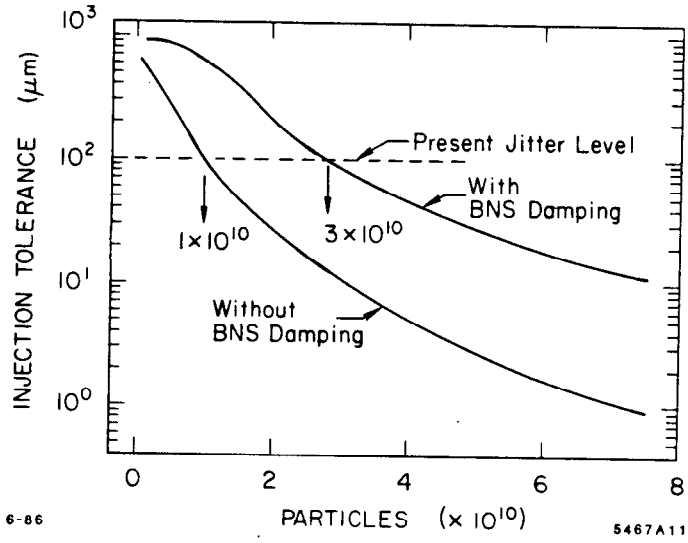

Fig. 5. Injection tolerance at linac input vs. beam intensity, with and without the application of BNS damping.

the Linac.[20] Other loops maintain constant position and angle input conditions[13] at the interface between major subsystems, *e.g.*, at injection from the RTL into the Linac, or in the beam switchyard (BSY), where e^- and e^+ beams are launched, respectively, into the North and South Collider Arcs (Fig. 1). Those loops, controlled either by dedicated microprocessors, or by the main VAX-8800 computer, operate on time scales of tens of milliseconds to minutes. More of those will be brought into operation as increased intensity and smaller spot sizes impose tighter constraints on machine performance.

D. Arcs

The SLC Arc system transports beams of electrons and positrons from the end of the Linac to the beginning of the Final Focus System, (FFS) where they are brought into head-on collision. To minimize phase-space dilution caused by quantum fluctuations in the synchrotron radiation energy loss mechanism, the bending radii are large; and very high-gradient, combined-function magnets are arranged in trains of low dispersion, terrain-following, densely-packed achromats.

A number of difficulties[21] that plagued early commissioning efforts have been overcome sufficiently well that the Arcs no longer significantly limit the machine performance.[22] Mechanical failures have been mended and gross betatron phase errors corrected[23] (Fig. 6). Adiabatic transitions at roll boundaries, spread over several magnets, have successfully suppressed (Fig. 7) cross-coupling of lattice dispersion caused

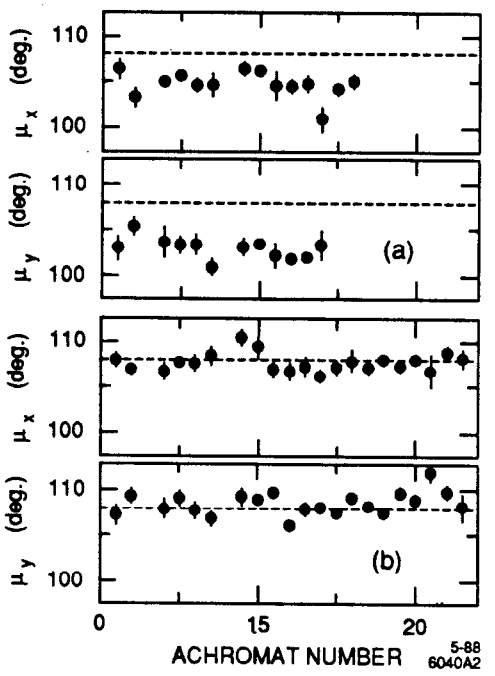

Fig. 6. Phase advances per cell in the South Arc (a) before, and (b) after correction.

by a combination of systematic gradient errors and abrupt transitions in the roll angle of the beam line.[24] Resonant betatron blowup has been tamed by exciting harmonic perturbations with a pattern of trim windings, to suppress damaging Fourier components in the errors at twice the betatron frequency.[25]

Residual errors in the alignment and field gradients of the Arc lattice, and systematic as well as random steering errors, still generate some cross-plane coupling, which must be corrected in the FFS. This increases the complexity of the overall tuning procedure and, if input horizontal and vertical emittances are unequal, results in dilution of the smaller of the two phase-space areas at the Arc output. Those effects are sufficiently small, however, that the degradation of the projected emittances does not exceed 25%. Continuing off-line analysis of measured betatron phase-space maps[26] will hopefully help bring the Arcs up to full SLC specifications in the next few months.

E. Final Focus System (FFS)

The FFS system contains the elements that demagnify the beams to a final spot size of a few μm, steer them into collision, and transport the spent beams to their respective dumps.

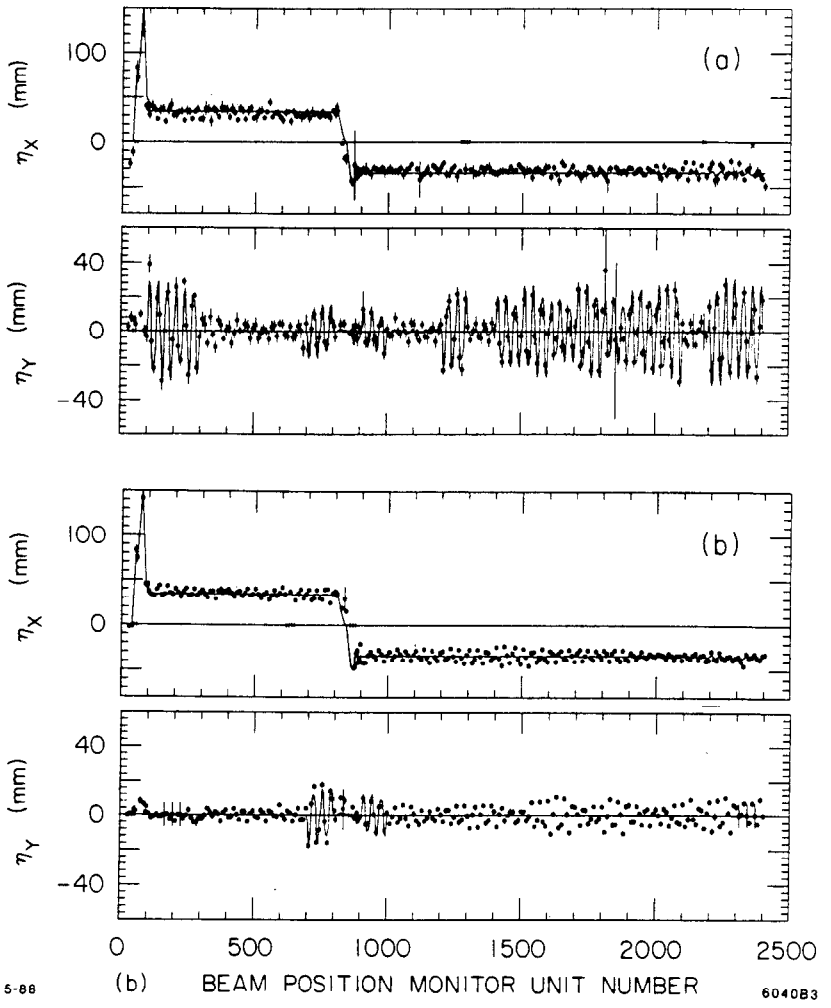

Fig. 7. Horizontal and vertical dispersion measured in the North Arc, (a) before, and (b) after the installation of the tapered roll transitions. The vertical dispersion was essentially suppressed by the modification.

The optical design[27] utilizes telescopic modules with simultaneous point-to-point and point-to-parallel focussing, to minimize the magnitude of higher order distortions.[21,28,29] More specifically, each arm (Fig. 8) consists of a dispersion-matching section, followed by a first level of demagnification which also completes, in betatron space, the matching of the incoming Arc beam. At this stage, most optical imperfections due to machine irregularities upstream have been corrected. The beam then traverses a chromatic correction section, whose purpose is to precisely balance the second-order chromatic aberrations induced by the high demagnification, short focal-length final telescope, without introducing geometric aberrations of comparable magnitude. For nominal incoming emittance, the design spot size at the IP is $\sigma = 2.4$ μm with the current optics.

One of the most severe challenges of linear colliders is to measure, and bring into collision, beams of the minute sizes needed to produce luminosity. While in storage

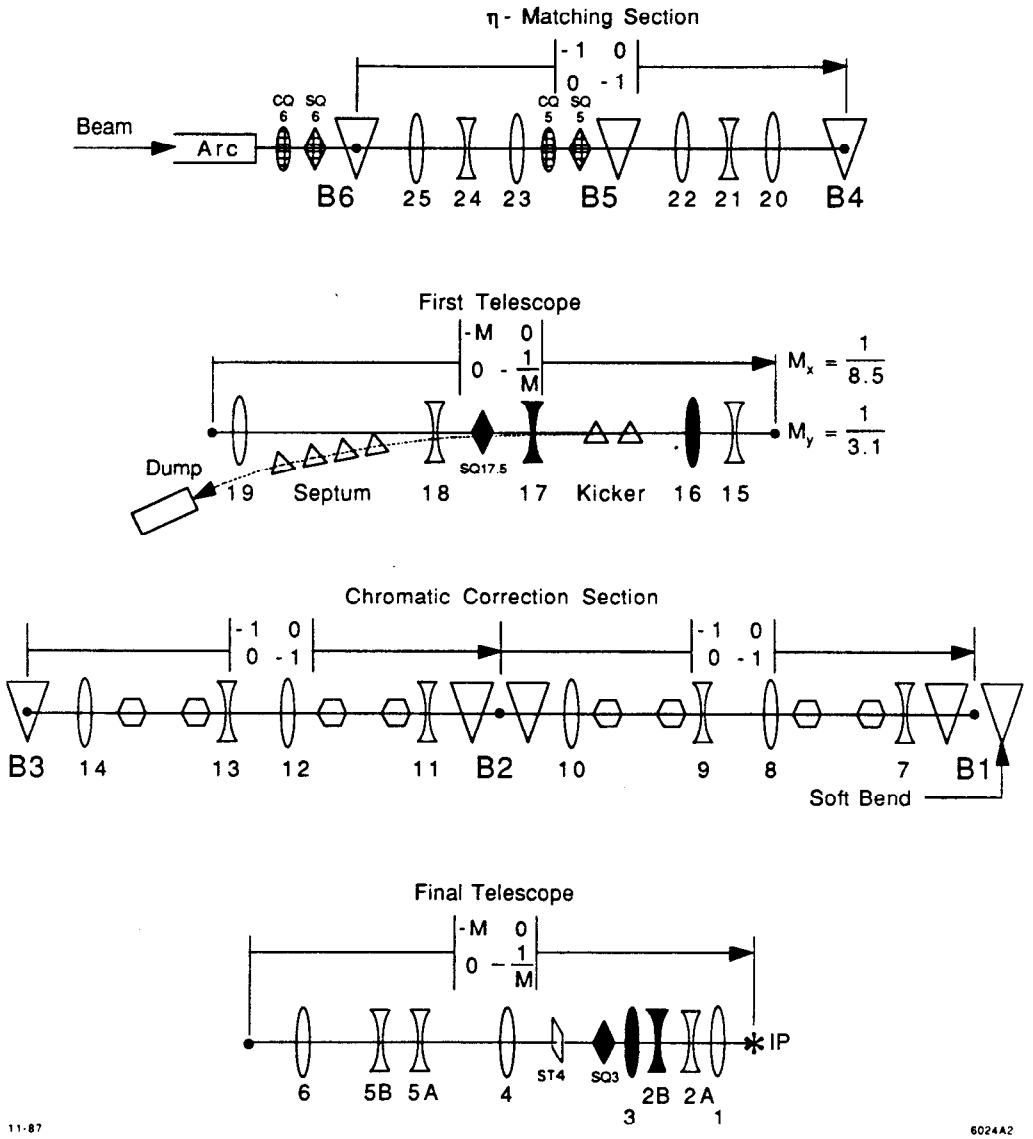

Fig. 8. Schematic of the Final Focus System. The four quadrupoles used for dispersion correction are shown cross-hatched, and the six quadrupoles used for betatron correction are shown shaded.

rings, constraints inherent to the machine itself almost force the beams into collision, no such recourse is available here. In addition, as the center-of-mass energy increases, the once prolific Bhabha scattering cross section no longer provides a sensitive enough luminosity monitor.

Single beam profiles have been measured[30] using thin carbon fibers scanning across the beam. Such a device is permanently installed inside the MarkII detector. It consists[31] of two wire-carrying heads at right angles to each other. Each head carries three wires (14, 3.5 and 2 μm in radius, respectively), and can be remotely "flipped" into the beam path. The beam is then scanned magnetically across one of the wires, producing secondary emission[30] and bremsstrahlung[32] signals proportional to the fraction of the beam intercepted. The heads are disposed such that one of them measures horizontal profiles, while the other head measures the vertical beam size. An example of the vertical positron beam profile at the IP is shown in Fig. 9.

Achieving such minute spot sizes requires that all components of transverse phase space, as well as the couplings between them, be carefully measured and controlled. An experimental tuning algorithm, supported by on-line optical matching packages,[33] has been successfully used to identify and diagnose the various betatron and dispersive contributions to the IP spot size.[34] Beam spots 3 to 5 μm wide are now routinely produced (Fig. 10). The horizontal spot size is limited by the larger than nominal Linac emittance; the vertical demagnification is limited to a larger than optimal β–function because of detector backgrounds. Near the end of the last run, vertical spot sizes very close to the design value have been repeatedly measured (Fig. 9), indicating that the optics of the FFS, including the delicate cancellation of higher order aberrations, behaves essentially as planned.

Let us now turn to beam-beam finding. The production of small, intense spots of electrons and positrons has made it possible to observe directly, for the first time, strong signals from the coherent interaction of the two beams. The deflection of one beam as it is scanned past the other[35] (Fig. 11) is detected by BPMs located inside the final lenses, that simultaneously measure both beams on each pulse and reconstruct the incoming and outgoing trajectories of each beam at each step of the scan. Beamstrahlung photons emitted during the deflection are detected[32] by a Čerenkov counter located downstream of the first bend in the outgoing orbit. Examples of these signals, taken simultaneously from a single sweep of the e^+ beam across the e^- beam, are shown in Fig. 12. Notice that the beamstrahlung flux is maximum—as expected, when the beam undergoes maximum

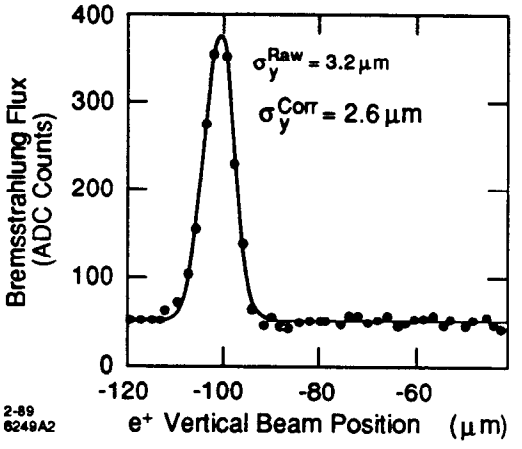

Fig. 9. Vertical positron beam profile at the SLC IP. The observed forward bremsstrahlung signal is plotted as the beam is scanned across a 3.5 μm radius carbon fiber in 2–μm steps. The raw measured R.M.S. beam size is 3.2 μm; the actual beam size, after deconvoluting the effect of the finite wire radius, is approximately 2.6 μm.

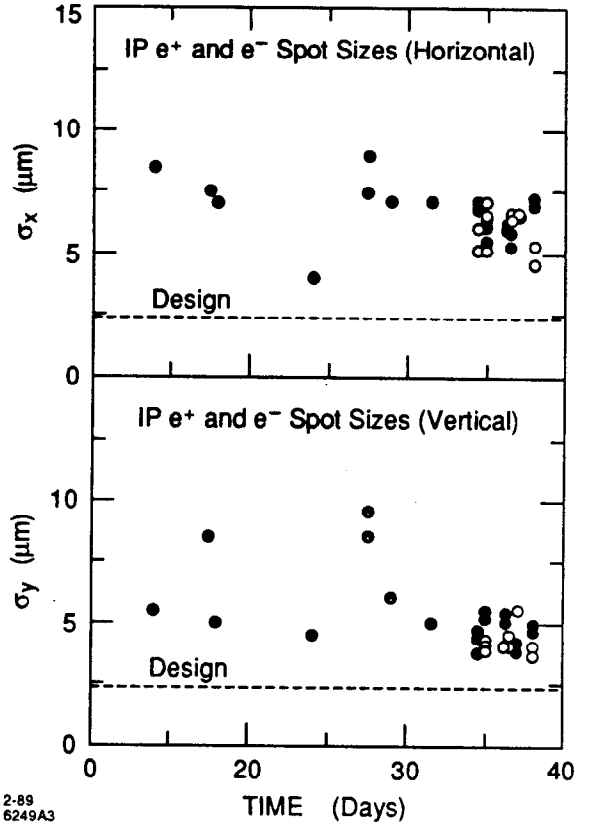

Fig. 10. History plot of horizontal and vertical electron beam sizes measured at the SLC IP. The effect of the finite wire radius (3.5 μm) has not been deconvoluted from the data.

deflection—and passes through a slight minimum when the beams collide exactly head-on, thereby reflecting the spatial dependence of the electromagnetic field generated by the other bunch.

The zero-crossing of the beam-beam deflection curve defines the precise location at which the two beams are properly aligned. On-line software is used to sweep the beams past each other, measure the beam-beam deflection to determine the zero-crossing, and to bring the two beams into collision. This procedure is sufficiently accurate to routinely maintain the beams aligned to better than 1 μm in both horizontal and vertical planes. Drifts in the beam-beam alignment have been monitored and found to be small enough that they can be corrected with suitable feedback loops.

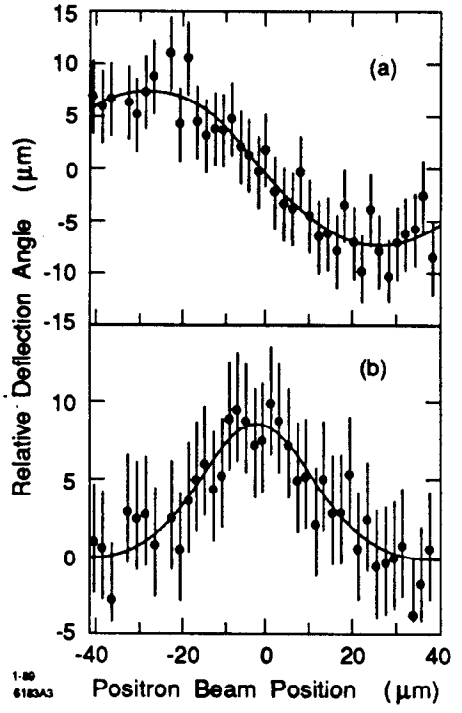

Fig. 11. The deflection of the e^+ beam as it is scanned past the e^- beam: (a) deflection in the plane of the scan, and (b) deflection in the plane perpendicular to the scan direction. When the beams are properly aligned, the deflection in the plane perpendicular to the scan will be zero, and the slope at the zero-crossing of the deflection in the plane of the scan will reach a maximum. The curves represent on-line fits to the data, assuming the beams are round.[35)]

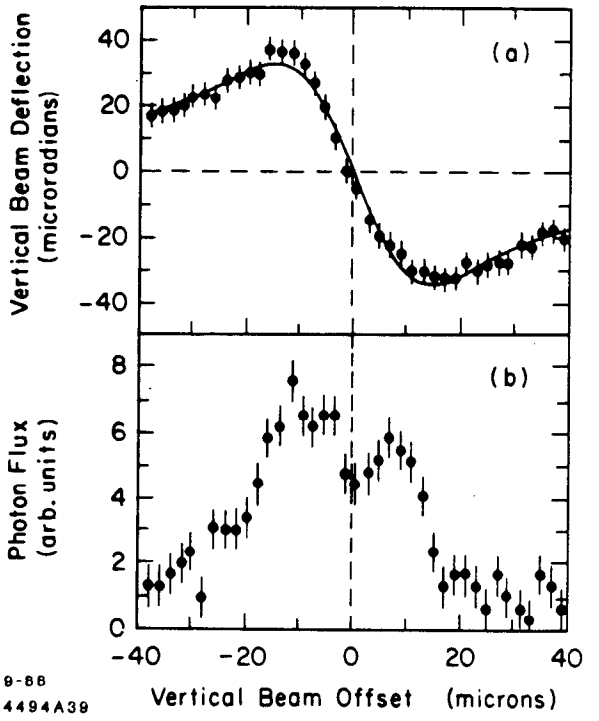

Fig. 12. Beam-beam deflection and beamstrahlung flux measurements taken simultaneously on a single scan of the e^+ beam past the e^- beam.

The magnitude and the detailed pattern of both the deflection[35)] and the beamstrahlung[36)] signals depend (in different ways for the two phenomena) on the beam currents, on the distance between the two beams, and on all six (longitudinal and transverse) beam sizes. They, therefore, constitute a very powerful set of diagnostics to optimize and monitor the luminosity.

F. Beam Collimation and Background Suppression

Electromagnetic debris, penetrating muons, and slow neutrons that are created when stray beam particles strike apertures in the FFS constitute backgrounds that, if sufficiently intense, will make it impossible for the experimental detector at the IP to acquire usable data. Elimination of these backgrounds requires extensive shielding and

protection of the detector, as well as efficient collimation of momentum and betatron tails sufficiently far upstream of the experiment.

In practice, it proved impossible to operate MarkII with primary collimation of the beam in the FFS itself, as originally planned. Tail electrons hitting collimators pair-produce muons through the Bethe-Heitler process. These muons are sufficiently abundant and penetrating to reach the detector and saturate its pattern recognition capability, if more than one electron in 10^4 is scraped within the FFS tunnel.

The muon flux through the detector has been controlled by the installation in the FFS of large toroidal magnets designed to deflect locally produced muons away from the detector and into the walls of the tunnel. In addition, the primary collimators were moved upstream of the FFS, into the Arcs and the BSY. The presently installed collimation scheme,[4] which has performed satisfactorily with beams of $\approx 10^{10}$ e^- and e^+ with the FFS optics set to $\beta^* \approx 4$ times the design value, will be complemented by an additional set of adjustable slits in the last sector of the Linac. These will provide complete and simultaneous collimation of both the electron and positron beams, and should be sufficient to allow operation at higher currents and smaller spot sizes.

IV. SUMMARY AND OUTLOOK

The SLC is the first of a new breed of facility that must be tamed if e^+–e^- collisions are to remain a tool for particle physics research much beyond the 100 GeV scale. The project has already shown that the linear collider principle is basically sound. It has produced crisp, original accelerator physics results. The most fundamental of these are the success of BNS damping and the first observation of beam-beam deflections and beamstrahlung, all of which are essential to the future success—or failure—of this new accelerator concept.

But the machine still needs to prove it can sustain a viable physics program at the Z°. Since last summer, a major effort, involving jointly particle and accelerator physicists, as well as most of the technical staff of the laboratory, has been undertaken to improve the reliability of operation. A large number of problems, affecting in particular the stability and reproducibility of magnetic configurations and of timing systems, have been identified and largely corrected. More systematic preventive maintenance is already paying off: the unscheduled down time in November was half of what it was in July. This Spring, after an initial period of recommissioning, the SLC will attempt to deliver beams of

about 2–3 $\times$ 10^{10} particles per pulse, of about 3 μm in size, at a repetition rate of 60 Hz. Most of those parameters stand within reach, or have already been achieved individually: the Z^0 production rate will depend critically on the overall efficiency.

On the longer term, the accelerator physics issues crucial to reaching the design instantaneous luminosity mostly concern "phase space control" in the Damping Rings and the Linac. Controlling bunch lengthening and beam tails much beyond intensities of 3×10^{10} will require major improvements in Damping Ring impedance, Linac alignment, kicker stability, and "wakefield management." Mastering these high currents is imperative in order to establish and maintain a significant particle physics program; it will also provide invaluable insight into the problems facing the next generation of linear colliders.

ACKNOWLEDGEMENTS

In preparing this talk, I have drawn on the work of many of my colleagues. I would like to thank in particular D. Burke, J. Clendenin, S. Ecklund, A. Hutton, N. Phinney, B. Richter, L. Rivkin, J. Seeman, J. Sheppard, and N. Toge, with whom I share the daily excitement of this enterprise. The masterful hand of A. De Rujula deserves the credit for the first illustration. I greatly appreciated the hospitality of Professor P. Strolin, chairman of this conference, and of his staff. I thank them for a lively and informative meeting in one of the most inspiring settings Italy has to offer.

REFERENCES

1. B. Richter and R. Stiening, The SLAC Linear Collider—A Status Report, SLAC-PUB-4367, invited talk presented by B. Richter at the 1987 Int. Sym. on Lepton and Photon Interactions at High Energies, Hamburg, Germany (1987).
2. V. Telnov, presented at the 1988 Workshop on Linear Colliders, SLAC, December 1988, Stanford, CA 94309, and references therein:
   I. Ginzburg, G. Kotkin, V. Serbo, V. Telnov, JETP 34(9) 491–5 (1981).
   I. Ginzburg, G. Kotkin, V. Serbo, V. Telnov, Nucl. Instr. Meth. 205, 47–68 (1983).
   I. Ginzburg, G. Kotkin, S. Panfil, V. Serbo, V. Telnov, Nucl. Instr. Meth. 219, 5–24 (1984).
   G. Kotkin and S. Polityko, Yad. Fiz. 34, 368–372 (February 1983), "The Possibility of Observing Production of Electron–Positron Pairs by a Photon in the Field of an Intense Electromagnetic Wave."
   C. Akezlof, Prep. UMHE, 81–59, 1981. Also SLC Workshop Notes–0039.
   A. Kondratenko, E. Pakhtusova, E. Saldin, Sov. Physics–DOKL (USA), Vol. 72, No. 6, p. 476–8 (June 1982), "Use of a Free–Electron Laser to Obtain High Energy

Colliding Photon Beams."
J. Spencer, SLAC–PUB–3645 (1985)

3. W. Kozanecki, Progress Report on the SLAC Linear Collider, Proc. of the Int. Europhysics Conf. on High Energy Physics, Uppsala, Sweden, June 1987.
4. D. Burke, The Stanford Linear Collider—Fall 1988, SLAC–PUB–4851, Invited paper, Meeting of the APS Division of Particles and Fields, Storrs, Connecticut, August 1988.
5. J. C. Sheppard *et al.,* Commissioning the SLC Injector, SLAC–PUB–4099, and Proc. of the 12th Particle Accelerator Conf., Washington, D. C. (March 1987).
6. J. E. Clendenin *et al.,* SLAC–PUB–4704, contr. to the 1988 Linear Accelerator Conf., (LINAC 88), Williamsburg, VA, 1988.
7. L. Rivkin *et al.,* SLAC–PUB–4645, contr. to the European Particle Accelerator Conf., Rome, 1988.
8. J. T. Seeman and J. C. Sheppard, Special SLC Linac Developments, SLAC–PUB–3944, 1986 Linear Accelerator Conf., Stanford, CA, 1986.
9. G. E. Fischer, SLC: Status and Development, SLAC–PUB–4012, Proc. of the Int. Conf. on High Energy Accelerators, Novosibirsk, U.S.S.R., August 1986.
10. J. T. Seeman *et al.,* Experimental Beam Dynamics in the SLC Linac, SLAC-PUB-4181, and Proc. of the 12th Particle Accelerator Conference, Washington, D.C. (March 1987).
11. R. Stiening, SLAC–PUB–4263, and Proc. of the 12th Particle Accelerator Conf., Washington, D. C. (March 1987).
12. M. Allen *et al.,* Performance of the Stanford Linear Collider Klystrons at SLAC, Proc. of the 12th Particle Accelerator Conf., Washington, D. C. (March 1987).
13. J. T. Seeman *et al.,* Transverse Wakefield Control in the SLC Linac, SLAC–PUB–4182, and Proc. of the 12th Particle Accelerator Conf., Washington, D. C. (March 1987).
14. J. T. Seeman *et al.,* invited talk presented at the 1988 Linear Accelerator Conf. (LINAC 88), Williamsburg, VA, 1988.
15. J. C. Sheppard *et al.,* invited talk presented at the 1988 Linear Accelerator Conf. (LINAC 88), Williamsburg, VA, 1988.
16. J. T. Seeman *et al.,* to be submitted to Phys. Rev. Lett.
17. K. Bane and T. Weiland, SLAC/AP–1, 1983.
18. R. Jobe *et al.,* SLAC–PUB–4703, contr. to the 1988 Linear Accelerator Conf. (LINAC 88), Williamsburg, VA, 1988.
19. V. Balakin, A. Novokhatsky and V. Smirnov, Proc. of the 12th Int. Conf. on High Energy Accelerators, Fermilab, 1983; K. Bane, SLAC/AP–69, 1988.
20. G. S. Abrams *et al.,* Fast Energy and Energy Spectrum Feedback in the SLC Linac, SLAC–PUB–4183, and Proc. of the 12th Particle Accelerator Conf., Washington, D. C. (March 1987).

21. P. Bambade, Recent Progress at the Stanford Linear Collider, SLAC–PUB–4610, invited talk presented at the 19eme Ecole de Physique des Particules, Marseille–Luminy, France, September 7–11, 1987.

22. T. Fieguth *et al.,* Tuning the Arcs of the SLAC Linear Collider, SLAC–PUB–4628, Contr. to the European Particle Accelerator Conf., Rome, 1988.

23. N. Toge *et al.,* A Technique for Correcting the Betatron Tunes of the SLC Arcs, to be presented at the 1989 Particle Accelerator Conf., Chicago, IL, March 20–23, 1989.

24. P. Bambade *et al.,* Rollfix—an Adiabatic Roll Transition for the SLC Arcs, to be presented at the 1989 Particle Accelerator Conf., Chicago, IL, March 20–23, 1989.

25. P. Bambade *et al.,* Wirefix—or Harmonic Corrections in the SLC Arcs, to be presented at the 1989 Particle Accelerator Conf., Chicago, IL, March 20–23, 1989.

26. T. Barklow, A Technique for Measuring the 4×4 Transfer Matrix for Beam Line Sections with Cross–Plane Coupling, to be presented at the 1989 Particle Accelerator Conf., Chicago, IL, March 20–23, 1989.

27. J. J. Murray, K. L. Brown, and T. Fieguth, The Completed Design of the Final Focus System, SLAC–PUB–4219, and Proc. of the 12th Particle Accelerator Conf., Washington, D. C. (March 1987).

28. K. L. Brown, A Conceptual Design of Final Focus Systems for Linear Colliders, SLAC–PUB–4159, and Proc. of the Joint US–CERN School on Particle Accelerators, South Padre, Texas, October 1986.

29. P. Bambade, Beam Dynamics in the SLC Final Focus System, SLAC–PUB–4227, and Proc. of the 12th Particle Accelerator Conference, Washington, D. C. (March 1987).

30. R. Fulton *et al.,* Nucl. Inst. and Meth. A274 (1989) 37.

31. G. Bowden *et al.,* Retractable Carbon Fibre Targets for Measuring Beam Profiles at the SLC Collision Point, SLAC–PUB–4744, 1989; submitted to Nucl. Inst. and Meth. A

32. G. Bonvicini *et al.,* A Monitor for Gamma Radiation at Zero Degrees from the SLC Collision Point, SLAC–PUB–4735, 1988. Submitted to Nucl. Inst. and Meth. A.

33. C. M. Hawkes and P. Bambade, First Order Optical Matching in the Final Focus Section of the SLAC Linear Collider, Nucl. Inst. and Meth. A274 (1989) 27.

34. P. Bambade *et al.,* Operational Experience with Optical Matching in the SLC Final Focus System, SLAC–PUB–4776, to be presented at the 1989 Particle Accelerator Conf., Chicago, IL, March 20–23, 1989.

35. W. A. Koska *et al.,* Observation of Beam-Beam Deflections at the Interaction Point of the SLAC Linear Collider, SLAC–PUB-4767, submitted to Phys. Rev. Lett.

36. P. Chen, private communication; G. Bonvicini *et al.,* in preparation.